

## Article

# Segmentation Differences of the Salt-Related Qiulitage Fold and Thrust Belt in the Kuqa Foreland Basin

Yingzhong Zhu <sup>1</sup>, Chuanxin Li <sup>1,\*</sup>, Yuhang Zhang <sup>2</sup>, Yibo Zhao <sup>1</sup> and Tulujun Gulifeire <sup>1</sup><sup>1</sup> School of Energy Resources, China University of Geosciences, Beijing 100083, China<sup>2</sup> School of Earth Sciences and Engineering, Xi'an Shiyou University, Xi'an 710065, China; yhzhang@xsyu.edu.cn

\* Correspondence: chuanxin\_li@cugb.edu.cn

**Abstract:** The Qiulitage fold and thrust belt (QFTB) is situated in the Kuqa Depression, exhibiting spectacular salt structures with well-defined geometric and kinematic characteristics and thereby playing a significant role in advancing the study of salt structures worldwide. This research, based on regional geology, well logging, and newly acquired three-dimensional seismic data, applies principles of salt-related fault structures to interpret seismic data and restore structural equilibrium in the Qiulitage fold and thrust belt within the Kuqa Depression by conducting quantitative studies on structural geometry and kinematics. Results indicate clear differences in salt structures between the eastern and western segments of it, vertically divided into upper salt, salt layer, and lower salt and horizontally into four parts. The Dina segment features a single-row basement-involved thrust fault, the East QFTB segment displays detachment thrust faults involving cover layers, the Central QFTB segment exhibits detachment thrust faults involving multiple rows of cover layers, the leading edge forms structural wedges, and the West QFTB segment develops blind-thrust faults. During the deposition of the Kangcun formation, the eastern profile experiences an 18% shortening rate, 14% in the central part, and 9% in the western part. For the Kuqa formation, the eastern profile experiences a 10% shortening rate, 9% in the central part, and 3% in the western part, indicating more significant deformation in the east than in the west. Quantitative statistical analysis reveals that different types of detachments, paleogeomorphology, and northeast-directed compressive stress exert control over the Qiulitage fold-thrust belt.

**Keywords:** Kuqa foreland basin; Qiulitage fold and thrust belt; salt structures; detachment layer; basement involvement structure



**Citation:** Zhu, Y.; Li, C.; Zhang, Y.; Zhao, Y.; Gulifeire, T. Segmentation Differences of the Salt-Related Qiulitage Fold and Thrust Belt in the Kuqa Foreland Basin. *Processes* **2024**, *12*, 1672. <https://doi.org/10.3390/pr12081672>

Academic Editors: Junjian Zhang and Zhenzhi Wang

Received: 14 June 2024

Revised: 23 July 2024

Accepted: 5 August 2024

Published: 9 August 2024



**Copyright:** © 2024 by the authors. Licensee MDPI, Basel, Switzerland. This article is an open access article distributed under the terms and conditions of the Creative Commons Attribution (CC BY) license (<https://creativecommons.org/licenses/by/4.0/>).

## 1. Introduction

Salt structures represent a significant type of basement structure widely occurring in various salt-bearing basins worldwide. Extensive research, such as field geological surveys, seismic interpretations, structural physics, and numerical simulations, indicates that the formation and evolution of salt structures in salt-bearing basins are primarily controlled by internal and external factors. The key controlling factors for salt structures vary greatly across different tectonic–sedimentary environments and evolutionary stages. Based on their contact relationship with surrounding rocks, salt structures can be classified into two types: passive diapirism and piercing diapirism [1–3]. In numerous seismic, drilling, and structural simulation experiments, it has been demonstrated that salt piercing through structures is a common phenomenon in rifts and passive margins of salt basins, such as the North Sea, Dead Sea, and Red Sea rifts, in northeastern Germany, Bohai Bay, and the Jiangnan Basin [4]. In contrast, thrust-related salt structures in compression-dominated salt basins, such as the Carpathian Basin, Zagros Basin, Amu Darya Basin, and Kuqa Depression, may exhibit remarkable characteristics, with salt-piercing structures being less common [2,5,6]. Sedimentary distribution of salt leads to the development of abundant salt-related structures within the Kuqa foreland basin. Over the past few decades, numerous

geologists have conducted extensive research on the styles and formation mechanisms of salt-related structures in the Kuqa foreland basin. Identified salt structure styles include salt anticlines, salt pillows, salt diapir, salt thrust sheets, allochthonous salt sheets, and overlying structures [7–10].

The Kuqa Depression boasts superior petroleum geological conditions, with the Qilitage fold and thrust belt being a secondary tectonic unit in the Tarim Basin [1,11–13]. Through years of research, the QFTB in the Kuqa foreland basin of the Tarim Basin has achieved significant breakthroughs in oil and gas exploration, led by well Mid-Autumn 1, with wells Dina 2 and Dina 11 also achieving notable success. However, there are also numerous examples of unsuccessful wells [14,15]. Through continued in-depth research, the salt-bearing structural features within the QFTB have become the focus of considerable attention. The geological structure of the QFTB exhibits pronounced east–west lateral segmentation, with significant layering characteristics vertically marked by salt formation [16]. However, due to the poor quality of early data and the influence of salt layers, there may be biases in the recognition of structural patterns, and quantitative statistics may be inadequate, particularly concerning the effects of different salt layers and the properties of Jurassic and Triassic detachment layers on fault formation, resulting in a lack of clarity in understanding. Therefore, in this study, building upon previous research and using regional geological information, we determine the sedimentary conditions of key formations in the study area, including the deposition of detachment layers and salt layers. Log data are utilized to establish the stratigraphy of seismic profiles. We combine the latest seismic data and apply principles of salt structure analysis to accurately delineate the geometric features of structures within the study area. Using 3Dmove inversion techniques, we establish a quantitative evaluation model for shortening, and we conduct a detailed analysis of the eastern segment of the QFTB, including a statistical analysis of data related to the fault width, fault dip angle, and detachment layer thickness. This study aims to provide a more refined analysis of it by highlighting its east–west differences, correlating thickness data of overlying and underlying detachment layers with structural patterns, and discussing causative mechanisms. This can lead to a better understanding of salt-bearing basins and help oil and gas exploration.

## 2. Geological Background

The Kuqa Depression, located in the transition zone between the southern Tianshan mountains and the Tarim Basin, belongs to the late Cenozoic intracontinental foreland basins [17,18]. It comprises several important structural units, including the Northern Structural Belt, the Kelaasu Structural Belt, the Qilitage fold and thrust belt, the Baicheng Depression, and the Yangxia Depression [8,19] (see Figure 1). Positioned at the coupling zone between the southern Tianshan mountains and the northern margin of the Tarim Basin, the Kuqa Depression, also known as the Kuqa foreland thrust belt, evolved as a retroforeland basin overlying the marginal foreland basin during the Mesozoic. Since the late Cenozoic, it has experienced intense compressional deformation, occurring from the Late Permian to the Quaternary. During the Pre-Cenozoic, the Kuqa Depression transitioned into a weakly extensional arid to semi-arid saline lake environment [20–22]. During the Paleogene to Neogene, the Baicheng Depression in the western and central parts of the Kuqa Depression served as the salt deposition center, shifting to the Yangxia Depression in the eastern part during the Miocene. This change in sedimentary centers resulted in varying thicknesses of salt formation within the Kuqa Depression, with the Kumugelm formation ( $E_{1-2}$ ) of the Paleogene having salt thicknesses ranging from 60 to 4000 m, and the Jidike formation ( $N_{1j}$ ) of the Miocene having salt thicknesses ranging from 240 to 1000 m, forming a complex array of salt-related structures [17,23–25]. The two sets of salt layers exert significant stratigraphic control on structural deformation between the upper and lower salt layers, leading to the formation of spectacular salt structures in the Kuqa Depression, with the most impressive salt structures developed in the Kelaasu Structural Belt and the Qilitage fold and thrust belt. The Neotectonic evolution of the

Kuqa Depression is mainly driven by north-to-south compressional forces induced by the uplift of the southern Tianshan Mountains, with a trend of increasing compression during the late Cenozoic [9,10,26,27].

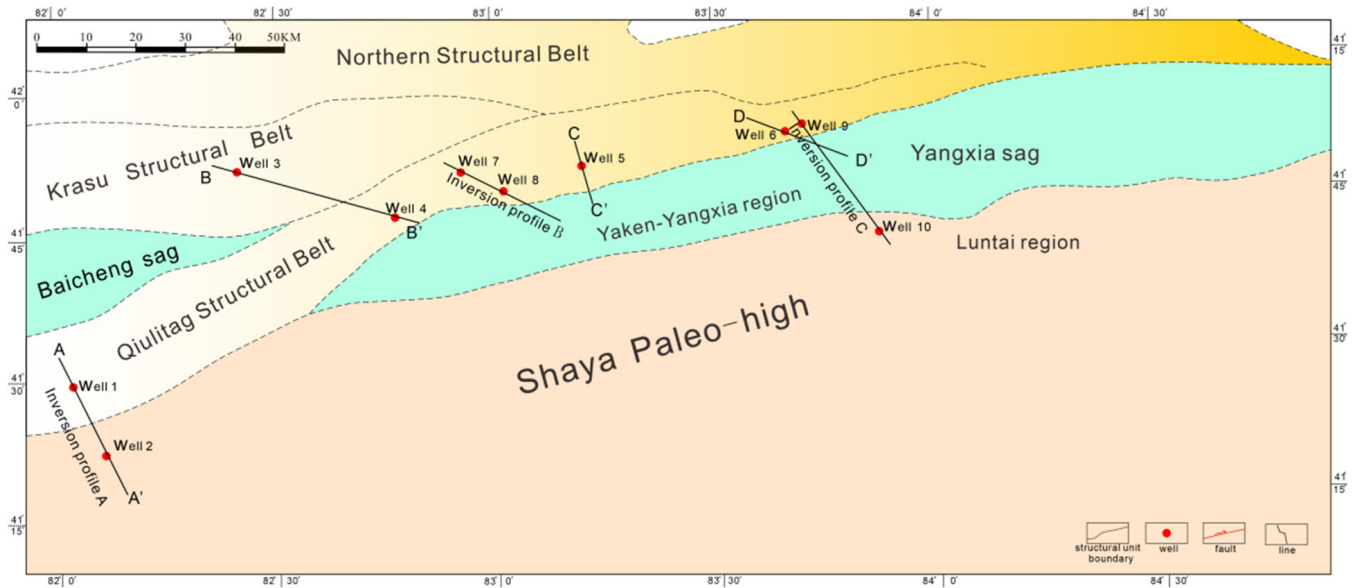


Figure 1. Geological cross-section location map of the Qiulitag fold and thrust belt.

The underlying formations beneath the salt formation in the Kuqa Depression primarily consist of the Upper Permian, Triassic, Jurassic, and Lower Cretaceous. Among these, the Upper Permian contains only one thick unit, the Biyoulebaogu formation (P<sub>2</sub>by), which is approximately 300 m thick. It comprises purplish-red sandy mudstone mixed with grey-green sandstone and fine conglomerate. It is angularly unconformable with the underlying Lower Permian or Carboniferous formations. The Triassic formations include the Ehuobulake formation (T<sub>1</sub>eh), the Kelamayi formation (T<sub>2-3</sub>k), the Huangshanjie formation (T<sub>3</sub>h), and the Taliqike formation (T<sub>3</sub>t), among others (see Figure 2).

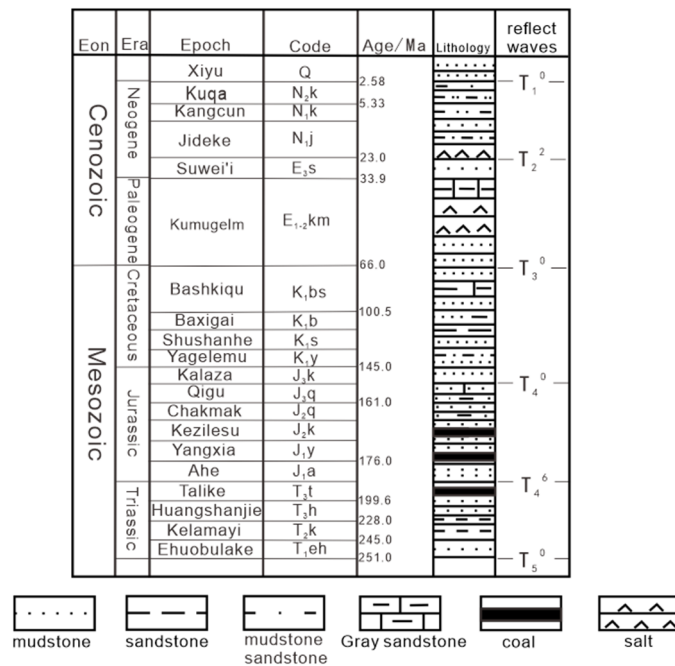


Figure 2. Distribution map of Mesozoic–Cenozoic layer in the Kuqa Depression [6].

The upper and lower layer of the Triassic exhibit different sedimentary environments; the lower part comprises purplish-red conglomeratic sandstone, grey-green sandstone, and mudstone deposited in alluvial fan and fluvial environments, while the middle to upper part consists of thick layers of grey-black mudstone and carbonaceous mudstone with coal interbedded, deposited in floodplain, nearshore lake, and deltaic environments. Overall, the sedimentary characteristics demonstrate a gradual thickening trend from the basin center towards the mountain belt, often displaying unconformable contacts with the underlying Triassic formations [6,24,28]. In the Kuqa Depression, the Upper Cretaceous is generally absent, while the Lower Cretaceous comprises conglomerate, sandstone, and mudstone interbedded, deposited in fan delta, braided river delta, and nearshore lake environments, including the Yagelemu formation ( $K_1y$ ), the Shushanhe formation ( $K_1sh$ ), the Basige formation ( $K_1b$ ), and the Bashkiki formation ( $K_1bs$ ). The Bashkiki formation is exposed in the western part of the northern monocline belt and in the Kelaasu and Yiqikeliq structural belts, representing the most important reservoirs in the Kuqa Depression. In the QFTB of the Kuqa Depression, thick layers of Mesozoic and Cenozoic layer have been deposited, influenced by the Paleogene uplifts, and extensively containing thick salt formation from the Paleogene Kumugelm formation ( $E_{1-2km}$ ) and Neogene Jidike formation ( $N_{1j}$ ) [29,30].

### 3. Structural Geometry Study

Building upon previous research, this study selects four well sections and combines actual drilling encounters, logging data, and interconnected well profiles to determine the distribution range of formations along the sections. Employing principles of salt-related fault analysis, the study conducts a detailed analysis of the sections and performs quantitative data statistics on certain parameters, such as the fault throw, dip angle, and thickness of detachment layers.

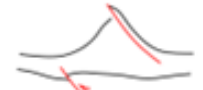
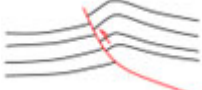
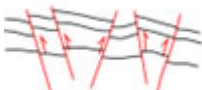
#### 3.1. Structural Geometry Characteristics

##### 3.1.1. Summary of Geometric Patterns

Building upon previous research, the region is divided into four parts, which are the western QFTB segment, the Central QFTB segment, the East QFTB segment, and the Dina segment. This study selects four well profiles and combines actual drilling encounters, logging data, and interconnected well profiles to determine the distribution range of formations along the sections. Employing principles of salt-related fault analysis, the study conducts a detailed analysis of the sections and performs quantitative data statistics on certain parameters, such as the fault throw, dip angle, and thickness of detachment layers.

Based on interpretations of numerous profiles from different locations within the study area, a synthesis of the geometric styles of the QFTB is presented. The upper salt layer primarily comprises two types: folding and faulting. Folding types include salt anticlines, mainly distributed in the western segment, while faulting types consist of fault-related folds and thrust faults, developed in the eastern segment of the QFTB. The salt layer mainly includes concealed piercing and piercing types. Concealed piercing types consist of dome-shaped and cap-shaped salt diapirs, developed in the western segment, while piercing types mainly comprise salt ridges, extensively developed in the eastern segment. The lower salt layer predominantly exhibits three structural styles: cover detachment, basement involvement, and block deformation. Cover detachment is mainly developed in the central and eastern segments, basement involvement primarily occurs in the Dina segment, and block deformation is predominantly observed in the western segment (see Table 1).

**Table 1.** Statistical table of structural styles in the Qiulitage fold and thrust belt.

Structure Layer	Type	Qiulitage Fold and Thrust Belt		Features
Upper Salt Layer	Fold Type	 Thrust-back fold	 Thrust-back fold	Shortening accommodated by folding, visible manifestation of growth strata phenomenon
	Fault Type	 Fault-bend fold	 Thrust block	Shortening accommodated by faulting, visible manifestation of growth strata phenomenon
Salt Layer	Blind Thrust Type	 Dome-shaped salt diapir	 Salt canopy	Salt layer in integral contact with surrounding rock
	Thrust Type		 Salt ridge	Salt intrusion into surrounding rock
Lower Salt Layer	Detachment Type	 Fault-bend fold	 Box fold	Salt-related fault along weak layer slip
	Basement-involved Type	 Thrust block	 Step fault block	Salt-related fault penetrates into the basement

### 3.1.2. Profile Analysis

In the typical profile A–A' of the western QFTB segment, located at the far western boundary of the study area (see Figure 1), three structural layers are delineated vertically based on the distribution of salt layers: the lower salt layer, the salt layer, and the upper salt layer. The lower salt layer primarily consists of a Cretaceous layer directly overlying the Cambrian layer, resulting in the absence of Triassic and Jurassic formations and the development of thrust faults caused by basement-cored folds. The salt layer comprises Paleogene salt formation, which exhibits a plastic flow influenced by late-stage structural activities, notably accumulating in well 1. Combining drilling data, the salt layer in well 1 can be divided into three segments, the upper salt rock segment, the middle mudstone segment, and the lower salt rock segment, with chaotic reflections in the upper and lower salt rock segments and strong continuous reflections in the middle mudstone segment. The upper salt layer primarily consists of Neogene formations, exhibiting significant thickness and influenced by late-stage compression, resulting in Y-shaped faults and secondary faults cutting through the salt layer. The folds in the upper salt layer are pronounced, with an evident growth layer observed in the Kangcun formation. In the planar view, previous data indicate a braided pattern, with multiple and relatively dense rows (see Figure 3).

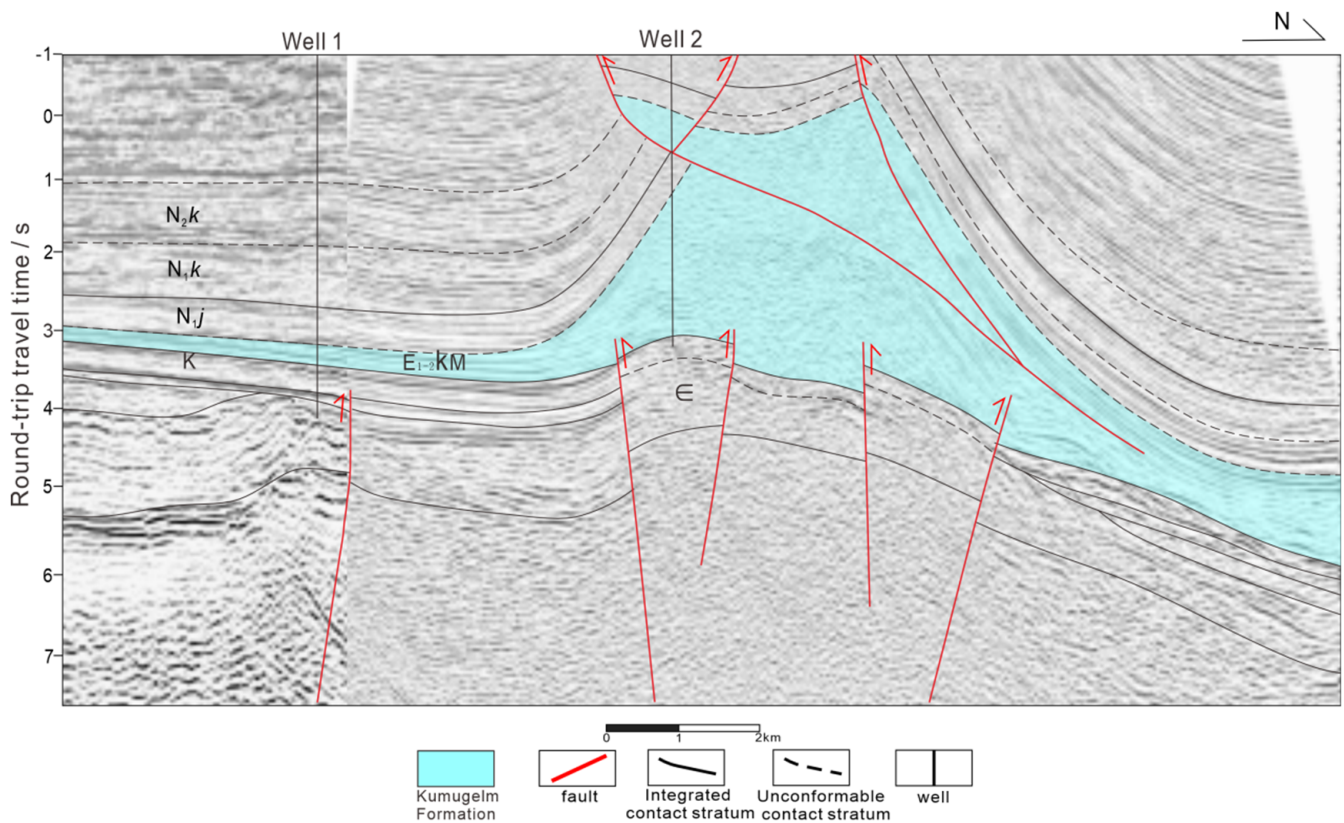


**Figure 3.** Typical section A–A' interpretation results of the western QFTB segment. Notes:  $N_2k$ –Kuqa formation;  $N_1k$ –Kangcun formation;  $N_{1j}$ –Jideke formation;  $E_{3s}$ –Suwei formation;  $E_{(1-2)km}$ –Kumugelm Group;  $K_1b$ –Bashkiqu formation; J–Jurassic; P–Triassic.

In the typical profile B–B' of the Central QFTB segment, located in the middle of the study area (see Figure 1), three structural layers are delineated based on the distribution of salt layers, belonging to the intersection of two salt lakes: lower salt, intermediate salt, and upper salt layers. The lower salt layer mainly consists of a Cretaceous layer, with Triassic and Jurassic mudstones serving as the primary detachment layers. The lower salt layer predominantly exhibits cover detachment-style thrust structures, with a fault dip angle of approximately  $15^\circ$ , a structural amplitude of 225 m, a structural width of 5.6 km, and a horizontal thrust distance of 0.7 km. The anticlinal closures are relatively gentle and extensive, while the Kelaasu Structural Belt features relatively steep and narrow anticline forms due to larger fault angles. The intermediate salt layer mainly comprises a salt formation from the Kumugelm formation ( $E_{1-2km}$ ) and a thick salt formation from the Jidike formation ( $N_{1j}$ ), as well as sandstones from the Suwei formation. The salt formations from the Kumugelm formation ( $E_{1-2km}$ ) are weakly developed in the central segment, showing a trend of pinch-out, while those from the Jidike formation ( $N_{1j}$ ) exhibit more deposition and clearer evidence of plastic flow. The upper salt layer primarily consists of Neogene formations, displaying distinct fold forms, with a notable growth layer observed in the Kangcun formation ( $N_{1k}$ ) (see Figure 4).

In the typical profile C–C' of the eastern segment passing through well 6 of the East QFTB segment, located in the central part of the study area (see Figure 1), the overall characteristics of the East QFTB segment are similar to those of the Central QFTB segment, with comparable structural layering. The Paleogene salt formations have already pinched out in the East QFTB segment, with only the salt formation from the Jideke formation being developed, serving as the boundary for stratification. The lower salt layer consists of Cretaceous, Jurassic, and Triassic formations, characterized by wide and gentle anticline-cored thrust faults. The fault dip angle is approximately  $12^\circ$ , with a structural amplitude of 287 m,

a structural width of 10.1 km, and a horizontal thrust distance of 6.3 km. Compared to the central segment, there are fewer rows of thrust faults, and the anticlines are incomplete, being cut by secondary faults. The leading edge of the lower salt layer does not develop primary thrust faults but rather secondary faults on the leading edge of the fault's lower wall. The salt formation in the East QFTB segment exhibits greater thickness, with plastic flow aggregation induced by late-stage compression (see Figure 5).

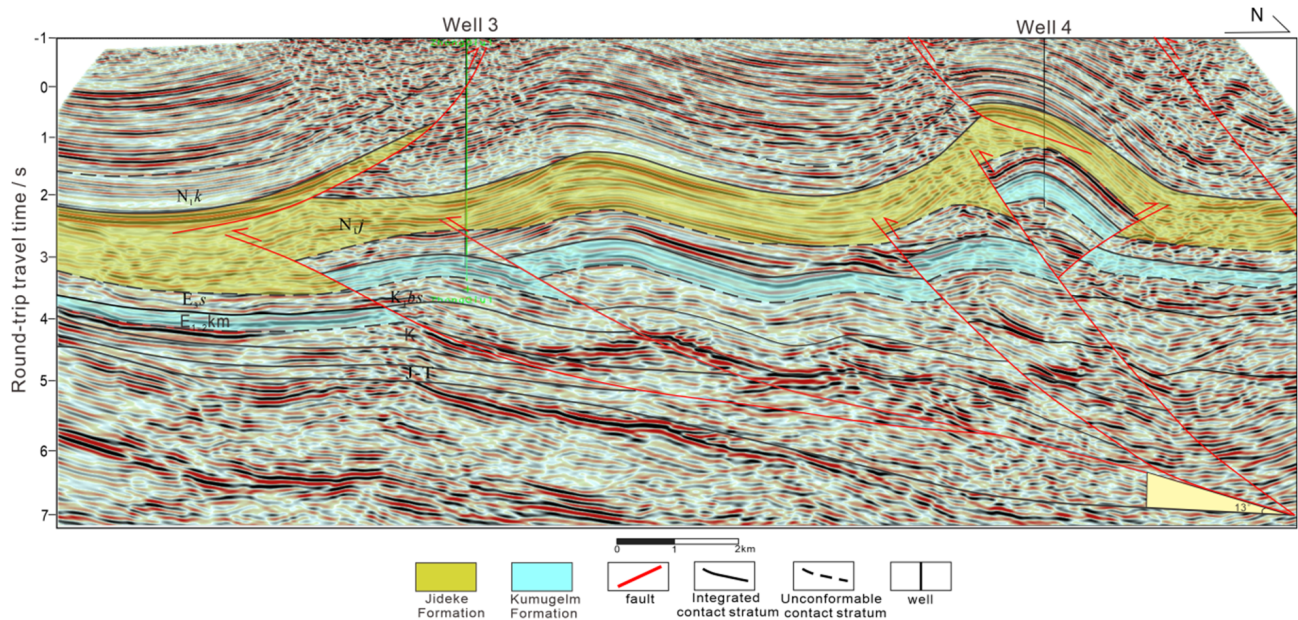


**Figure 4.** Typical section B-B' interpretation results of the Central QFTB segment. Notes: N<sub>2</sub>k–Kuqa formation; N<sub>1</sub>k–Kangcun formation; N<sub>1</sub>j–Jideke formation; E<sub>3</sub>s–Suwei formation; E<sub>(1–2)</sub> km–Kumugelm Group; K<sub>1</sub>b–Bashkiqu formation; J–Jurassic; P–Triassic.

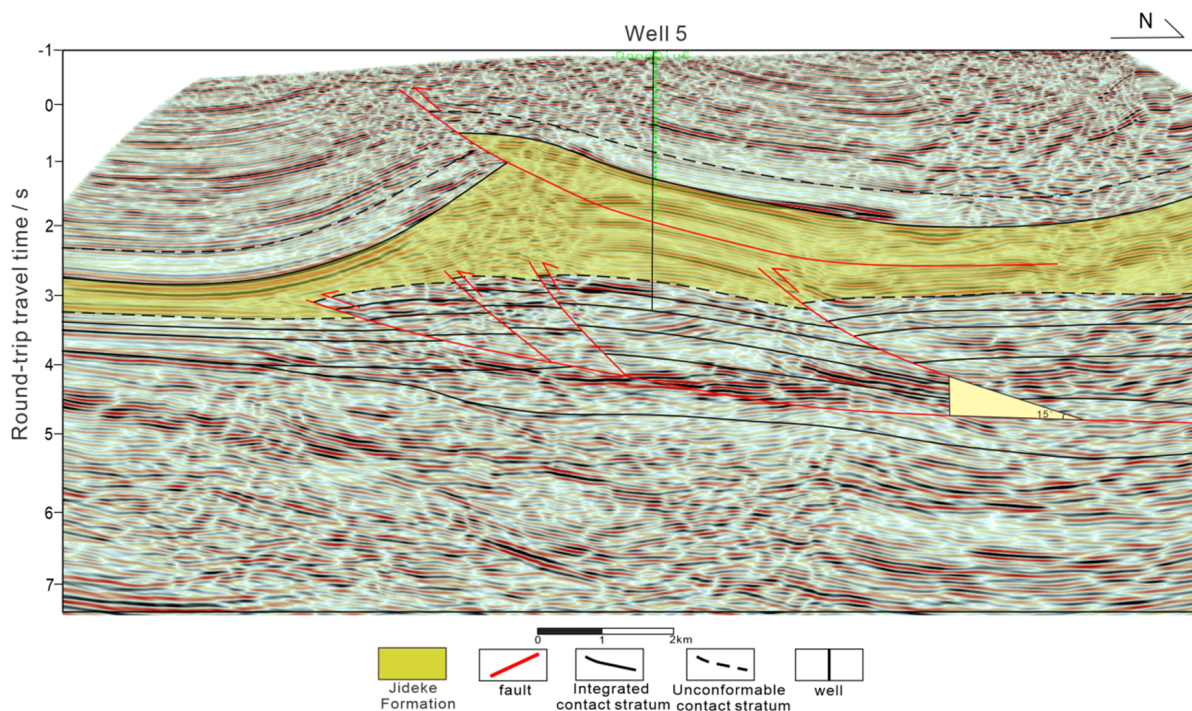


**Figure 5.** Typical section C-C' interpretation results of the East QFTB segment. Notes: N<sub>2</sub>k–Kuqa formation; N<sub>1</sub>k–Kangcun formation; N<sub>1</sub>j–Jideke formation; E<sub>3</sub>s–Suwei formation; E<sub>(1–2)</sub> km–Kumugelm Group; K<sub>1</sub>b–Bashkiqu formation; J–Jurassic; P–Triassic.

In the typical profile D–D', located in the eastern part of the study area (see Figure 1), it represents the easternmost end of the QFTB. The Dina segment only hosts a single set of salt formations from the Jideke formation. Beneath these, there are Cretaceous, Jurassic, and Triassic formations, characterized by a single row of basement-involved thrust faults. The fault dip angle is approximately 30°, with a structural amplitude of 375 m, a structural width of 6.2 km, and a horizontal thrust distance of 3.5 km. The angle notably increases, presenting an overall morphology in the shape of an inverted Y. The form of the anticline in the lower salt layer is intact, facilitating good preservation of oil and gas. The folding morphology in the upper salt layer is relatively weaker, with an observable growth layer in the Kangcun formation (see Figure 6).

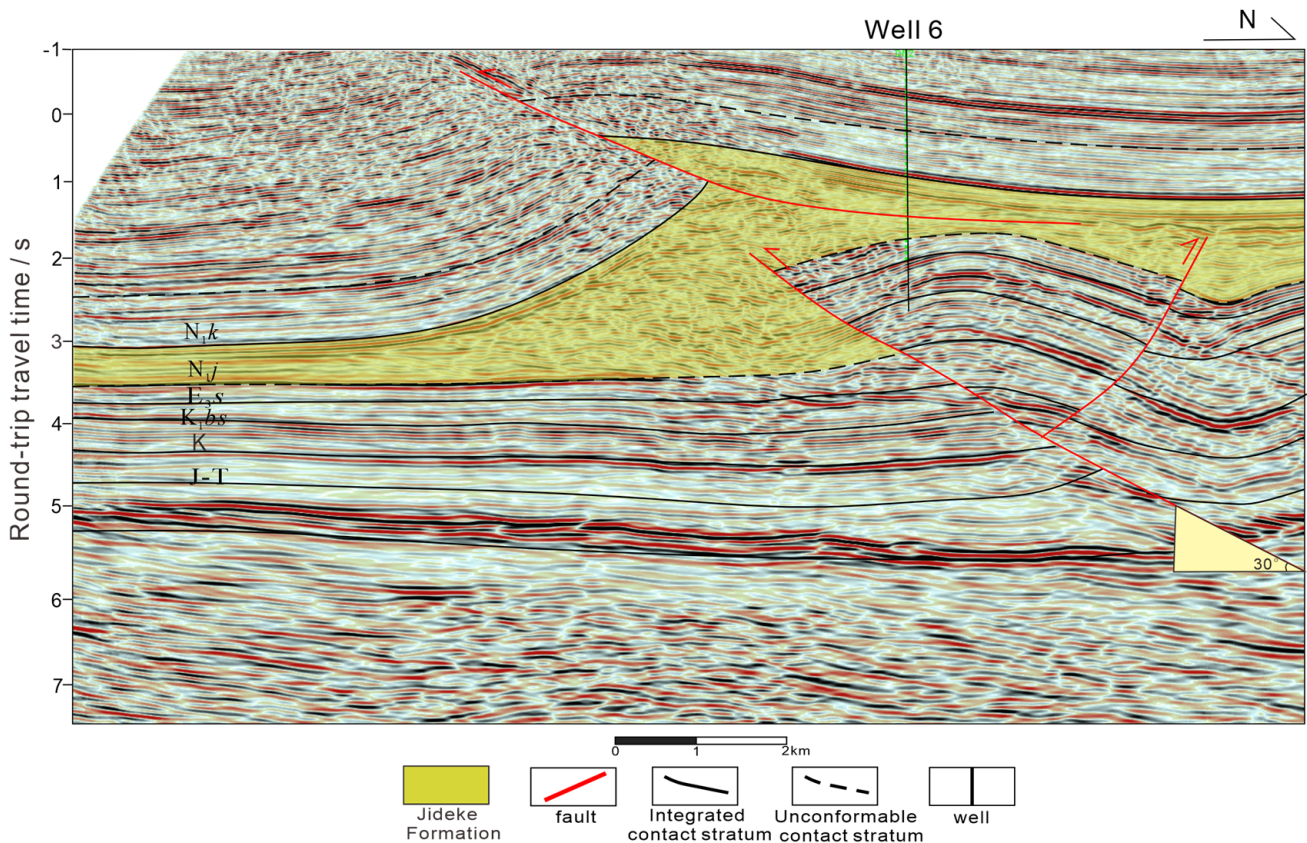


**Figure 6.** Typical section D–D' interpretation results of the Dina segment. Notes: N<sub>2</sub>k–Kuqa formation; N<sub>1</sub>k–Kangcun formation; N<sub>1</sub>j–Jideke formation; E<sub>3</sub>s–Suwei formation; E<sub>(1–2)</sub>km–Kumugelm Group; K<sub>1</sub>b–Bashkiqu formation; J–Jurassic; P–Triassic.

### 3.2. Planar Characteristics of the Qiulitage Fold and Thrust Belt

Building upon previous research and the latest data interpretations, the planar distribution characteristics of the QFTB in the study area have been summarized.

In the study area, the QFTB shows a northeast trend in its sub-salt fractures, not an east-west orientation. Convergence in the east gradually transitions to divergence in the west. Fault zones progress from single-row in the east to double-row and multi-row in the central area, eventually leading to nearly vertical multi-row faults in the west (see Figure 7).

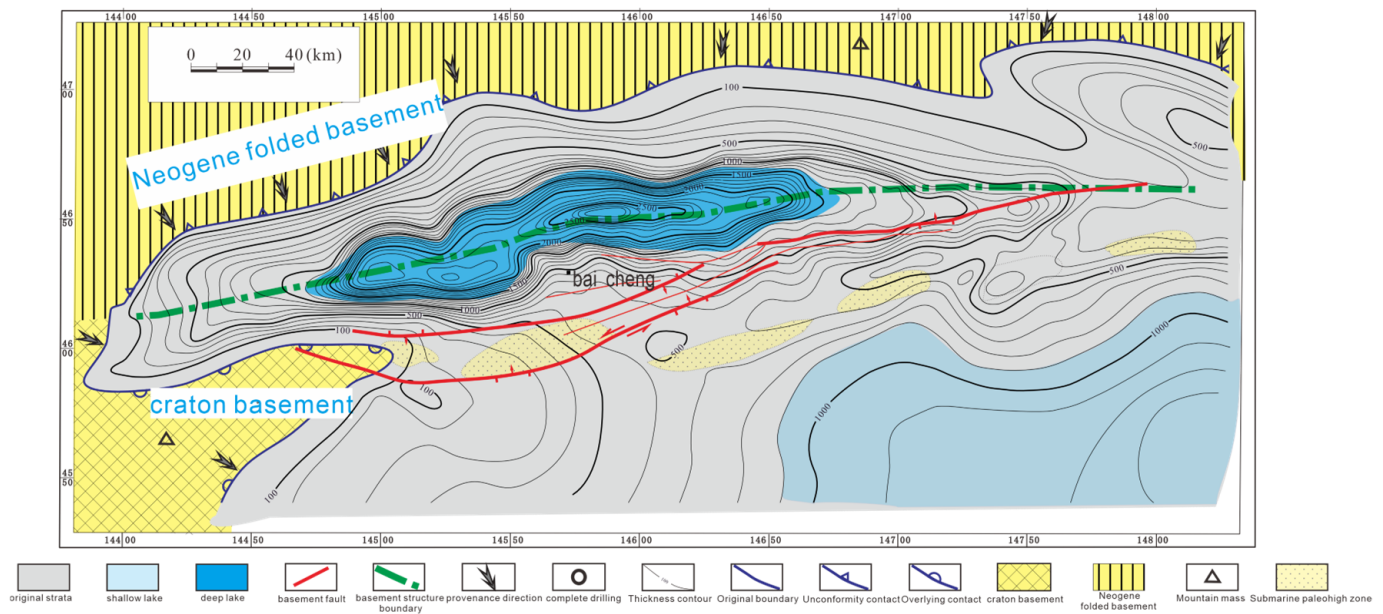


Figure 7. Paleogeographic map of the Cretaceous in the Kuqa Depression [13].

#### 4. Structural Kinematic Characteristics Study

This paper utilizes Move 2018 software to perform balanced restoration on five profiles within the working area that are nearly perpendicular to the structural trend. During the restoration process, the principles of layer length and area conservation are followed. The formation units are divided into upper and lower segments along the top surface of the salt formation sequence to minimize the effects of deformation caused by the salt formation. The restoration of balanced profiles mainly involves two steps: gap removal and layer flattening. For typical reverse fault systems, the gap removal is initially performed using the kinematic fault-parallel flow (Flexural slip unfold) restoration technique, followed by layer flattening using the non-kinematic flexural slip unfold technique to remove folds, restoring them to a reference plane (Restore). Before and after profile restoration, a comparison of the formation line lengths is conducted to prevent significant errors. Through quantitative analysis of the evolution of balanced profiles, the shortening rates at different locations and periods are calculated.

In this study, three profiles were selected for inversion in the western, central, and eastern sections of the QFTB in the study area, named, respectively, the western inversion profile, the central inversion profile (see Figure 1), and the eastern inversion profile, using Move 2018 software for balanced restoration.

The western profile is divided into upper and lower layers based on the top boundary of the Neogene Kumugelm formation for balanced restoration (see Figure 8). Before the deposition of the Kumugelm formation, the western region experienced basic formation of the ancient uplift, with significant sedimentary hiatuses observed in the Triassic layer. The upper layers above the ancient uplift exhibit severe formation gaps, with the Cretaceous layer deposited directly above the Cambrian layer. Until the deposition of the Kuche formation, it was a period of tectonic quiescence. Following the deposition of the Kangcun formation, block-like structures appeared in the lower salt-bearing layer, while the upper salt-bearing layer exhibited severe folding deformation, forming dome-like structures with a shortening rate of 9%. The faults have been active to the present day, with increased displacement of lower salt-bearing blocks and intensified folding deformation of upper salt-bearing layer, accompanied by the development of a secondary fault with an opposite dip, resulting in a shortening rate of 3%.

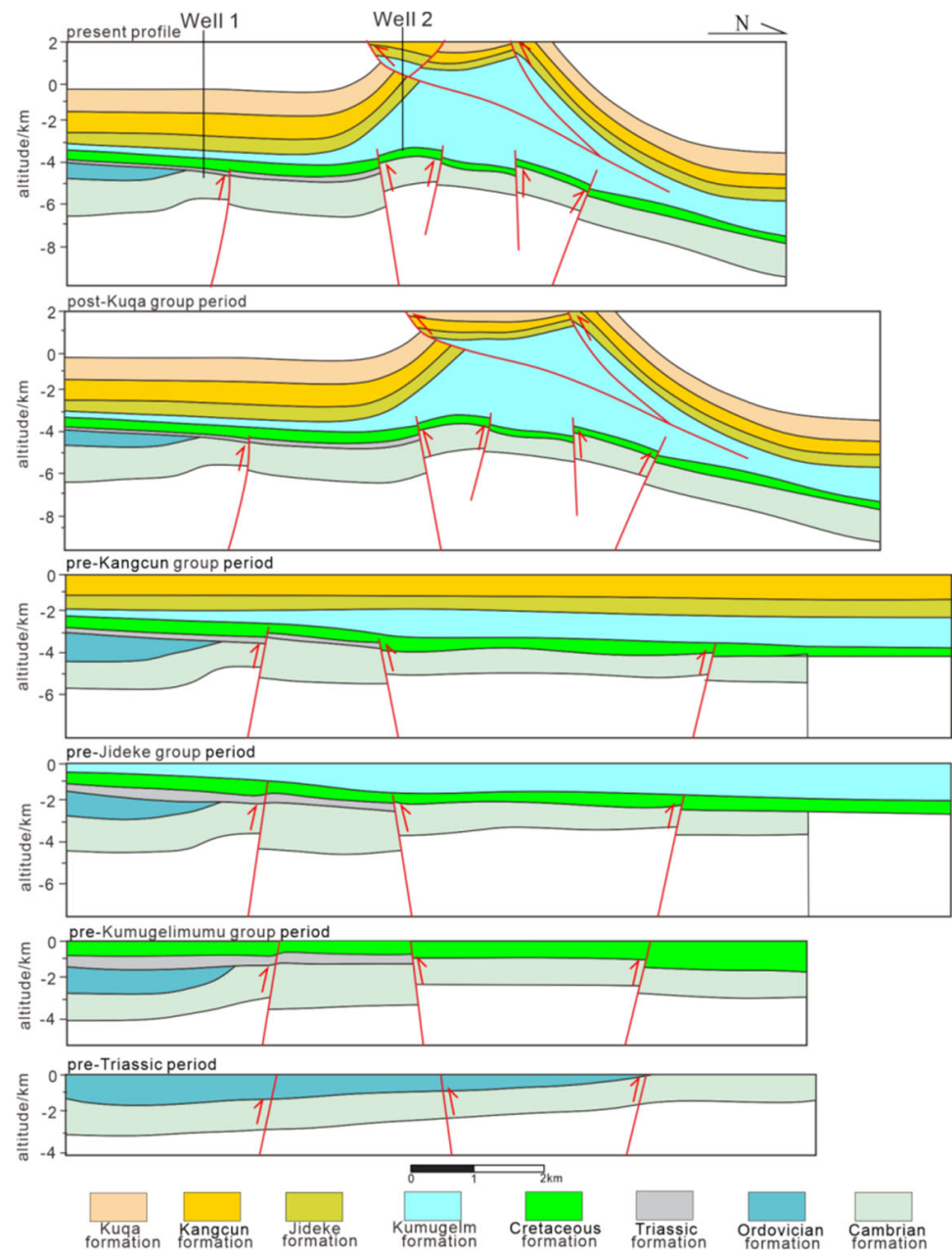


**Figure 8.** Evolutionary results of the western profile.

The central profile is divided into upper and lower layers based on the top boundary of the Neogene Jideke formation for balanced restoration. Before the deposition of the Kangcun formation, it was a period of tectonic quiescence. Influenced by ancient uplift, the Triassic layer in the northern part experienced thicker sedimentation than in the southern part. After the deposition of the Kuche formation and before the Kangcun formation, thrust faults began to develop nearly simultaneously in the lower salt-bearing layer, forming a stack-style thrust fault system. The upper salt-bearing layers were also simultaneously active, forming fault bend folds with a shortening rate of 14%. Fault activity continues to the present day, with the development of a set of opposite-dipping back thrust faults in the northern front, intensifying the folding deformation of the upper salt-bearing layer, with salt layers extruding to the surface, resulting in a shortening rate of 9% (see Figure 9).

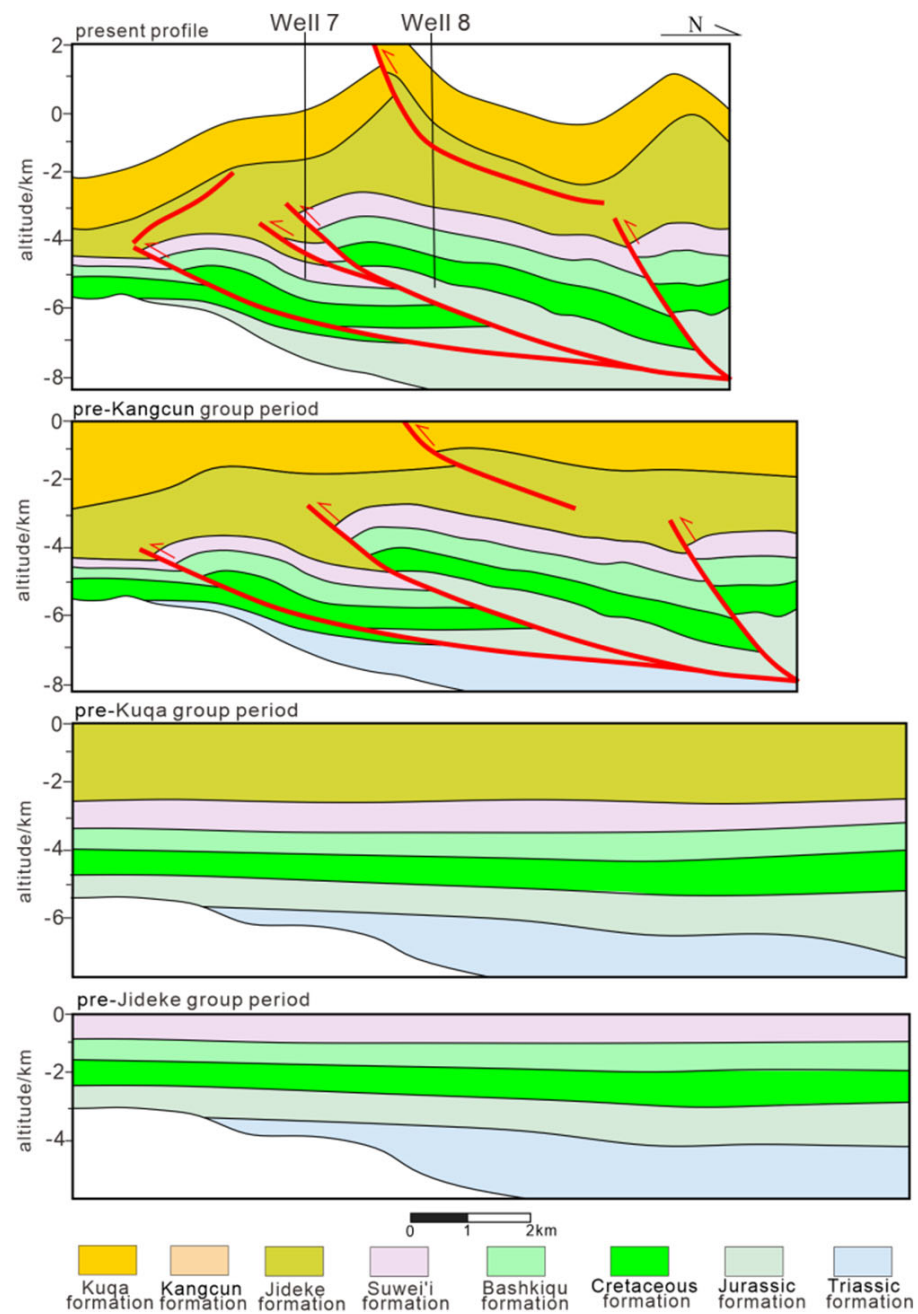


**Figure 9.** Evolutionary results of the central profile.

The eastern section extends to the Yakra Bulge in the south, the Northern Structural Belt in the north, and the QFTB in the middle. The eastern profile is divided into upper and lower layers based on the top boundary of the Neogene Jideke formation for balanced restoration. Before the deposition of the Cretaceous layer, the faults in the northern fold-and-thrust belt became active, developing forward thrust faults with a shortening rate of 10%. After the deposition of the Cretaceous layer, the faults in the northern fold-and-thrust belt continued to develop. Before the deposition of the Kangcun formation, the Qiulitage fault became active with a shortening rate of 18%. After the deposition of the Kuche formation, the faults continued to develop with a shortening rate of 10% (see Figure 10).

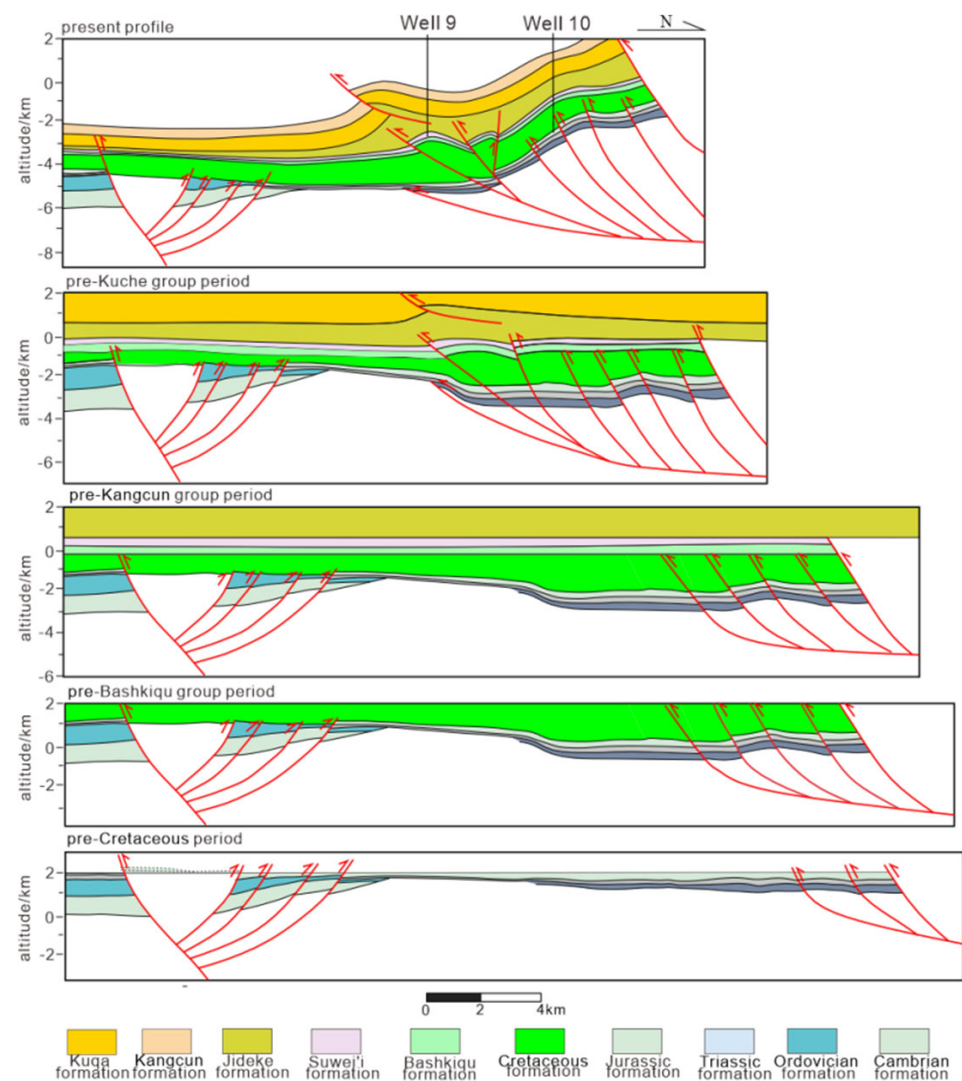


**Figure 10.** Evolutionary results of the eastern profile.

Although there are significant differences in the fault styles between the eastern and western sections of the QFTB, based on the variations in shortening rates, the deformation periods are generally before the deposition of the Kuche formation and continue to the present day, indicating that the Xishan period is the main deformation period of the QFTB. However, the shortening rate in the western section is generally less than 10%, while in the central inversion profile, the shortening rate during the main deformation period is greater than 10%, and in the eastern inversion profile, the shortening rate during the main deformation period is even greater, indicating more intense deformation. It can be observed that the deformation intensity of the QFTB gradually weakens from east to west (see Table 2 and Figure 11).

**Table 2.** Statistical table of shortening-rate-related parameters.

Profile	Pre-Kangcun Group Period	Pre-Kuqa Formation Deposition	From the Kuqa Formation to the Present
Western profile	14.90 km	13.56 km	13.15 km
Middle profile	13.96 km	12.01 km	10.93 km
Eastern profile	30.18 km	24.75 km	22.28 km

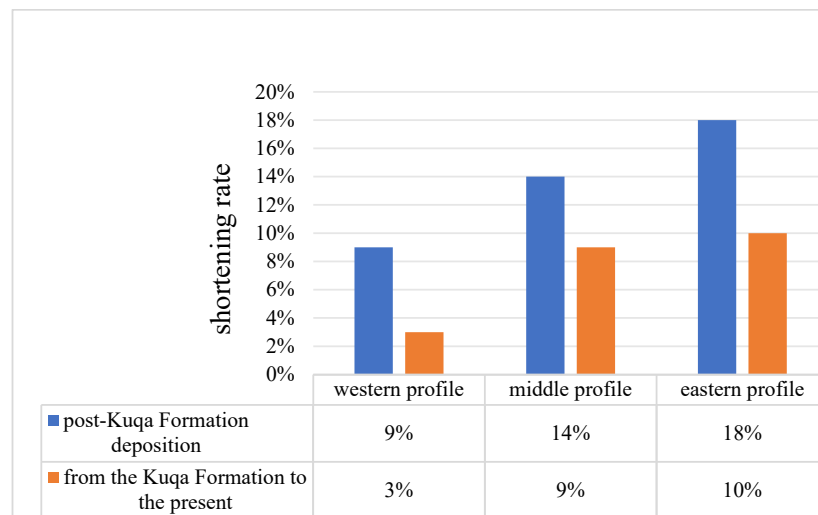


Figure 11. Statistical table of profile shortening ratios.

### 5. Differential Analysis of the Qiulitage Fold and Thrust Belt

Building upon previous work, we have summarized the reasons for the east-west differences in the QFTB, mainly reflected in two aspects: the variability in detachment layers and the variability in stress fields.

Firstly, the detachment layers in the study area primarily consist of two sets: the upper detachment layer, comprising the Kumugelm formation’s salt formation, mainly distributed in the western section but extinguished in the central section, and the salt layer of the Neogene Jideke formation, mainly distributed in the eastern section of the QFTB. The lower detachment layer consists of Jurassic and Triassic mudstones, primarily distributed in the eastern section of it but extinguished in the western section (see Figures 12 and 13).

Based on the distribution and geometric characteristics of the salt layers, it is divided into four segments: the West QFTB segment, the Central QFTB segment, the East QFTB segment, and the Dina segment. The Central QFTB segment is where the two salt lakes converge, with the gypsum-salt layer of the Kumugelm formation gradually extinguishing and the new salt formation of the Jideke formation beginning to develop. In this segment, the lower salt layer develops multiple layers of cover detachment thrust structures, while the upper salt layer develops thrust fault blocks. The East QFTB segment only develops the salt formation of the Jideke formation, with broad and gentle cover detachment double-row thrust structures, and the upper salt layer develops thrust folds. Similarly, the Dina segment also only develops the salt formation of the Jideke formation, with single-row high-angle basal-involved thrust structures and thrust folds in the upper salt layer.

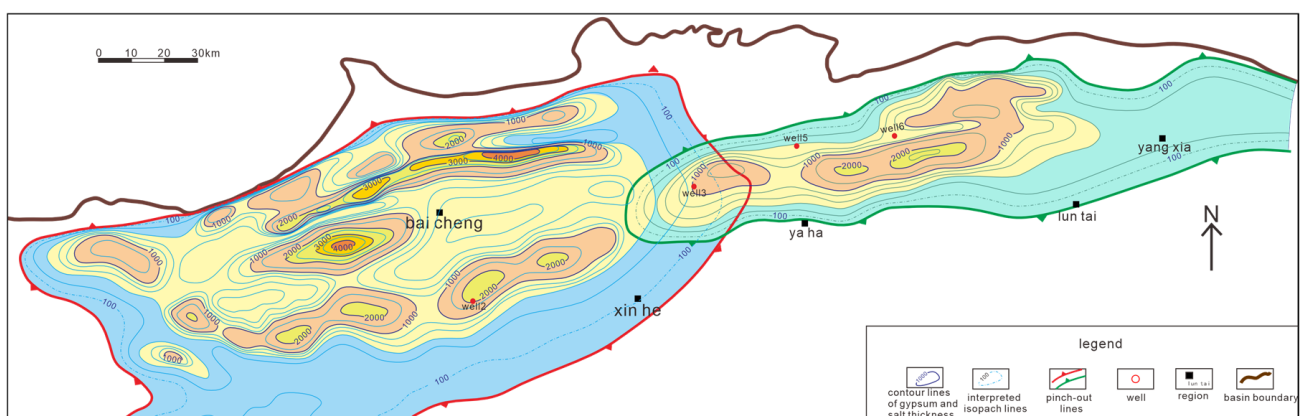
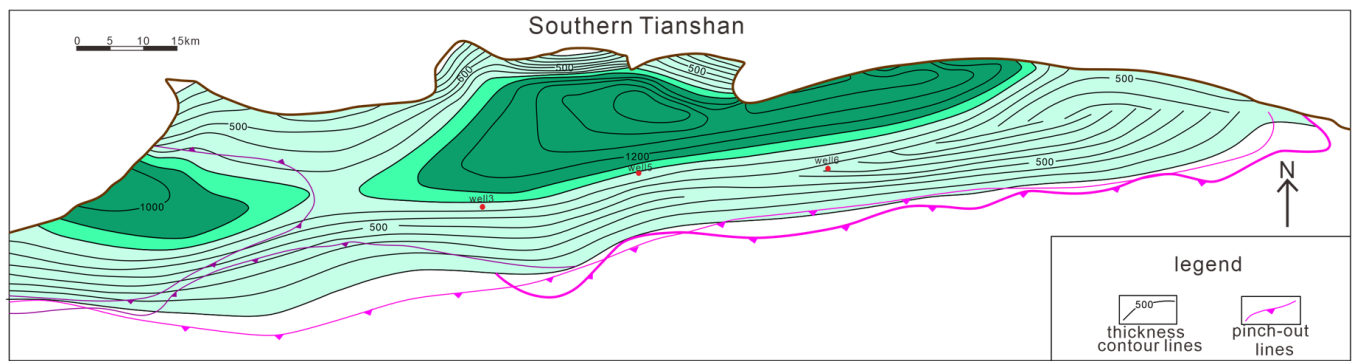


Figure 12. Contour map of thickness distribution of Paleogene and Neogene salt layers [7].



**Figure 13.** Contour map of thickness distribution of Jurassic and Triassic mudstones [16].

According to statistical data, the type and thickness of the upper detachment layer determine the number of faults in the fault belt, while the thickness of the lower detachment layer determines the development mode of the faults. Overall, the thickness of the Jurassic and Triassic detachment layers in the central to eastern segments is greater than 800 m, whereas in the Dina segment it is less than 800 m. Therefore, when the thickness of the Jurassic and Triassic detachment layers exceeds 800 m, cover detachment thrust faults develop, whereas when the detachment layer thickness is less than 800 m, basal-involved thrust faults develop. In the absence of a lower detachment layer, imbricate thrust faults do not develop (see Table 3).

**Table 3.** Statistical table of comparative analysis of profile feature differences.

Profile	The Thickness of the Detachment Layer in the Jideke	The Thickness of the Detachment Layer in the Kumugelm	The Thickness of the Detachment Layer in the Jurassic–Triassic Layer	Fault Development Mode	Fault Dip Angle	Number of Faults	Horizontal Thrust Distance
A–A′	0 m	2000 m	\	Fault block type	\	Multiple rows	\
B–B′	1000 m	150 m	800 m	Cover detachment type	12°	Three rows	0.7 km
C–C′	800 m	0 m	1000 m	Cover detachment type	15°	Double rows	6.3 km
D–D′	600 m	0 m	600 m	Basement-involved type	30°	Single row	3.5 km

In the eastern part closer to the orogenic belt, stress is stronger, resulting in more intense deformation, while in the western part farther from the orogenic belt, stress is relatively weaker. From the statistical data, it can be observed that the dip angles of faults in the central to eastern segments are significantly smaller than those in the Dina segment, with dip angles ranging from 12° to 15° in the central to eastern segments and around 30° in the Dina segment. Combined with the statistical results of the shortening rates from the inversion profiles, it can also be inferred that the eastern part closer to the orogenic belt experiences more intense fault activity. The horizontal thrust distance should be jointly determined by the detachment layer and stress conditions.

In the late Miocene, the Indian Plate accelerated its subduction towards the Eurasian Plate, causing rapid uplift of the Southern Tianshan Mountains and exerting north-to-south compressive stress on the Kuqa Depression. This marked the Kuqa Depression's transition into the stage of a regenerated foreland basin. The complex compressive salt structure deformations seen today primarily formed during this period. As shown in the pattern diagram, the compressive stress from the Southern Tianshan Mountains, along with the uplift of the orogenic belt, provided a north–eastward compressive stress field, resulting in high-angle basal-involved faults in the Dina segment. However, as stress relatively weakened and under the influence of the lower detachment layer, low-angle multiple-row imbricate thrust fault systems appeared in the central to eastern segments. At the forefront of the salt lake convergence zone in the upper detachment layer, a back thrust fault formed, while in the West QFTB segment, as stress continued to decrease, the thrusting action did

not persist, and the imbricate thrust fault system did not continue, only forming multiple block faults (see Figure 14).

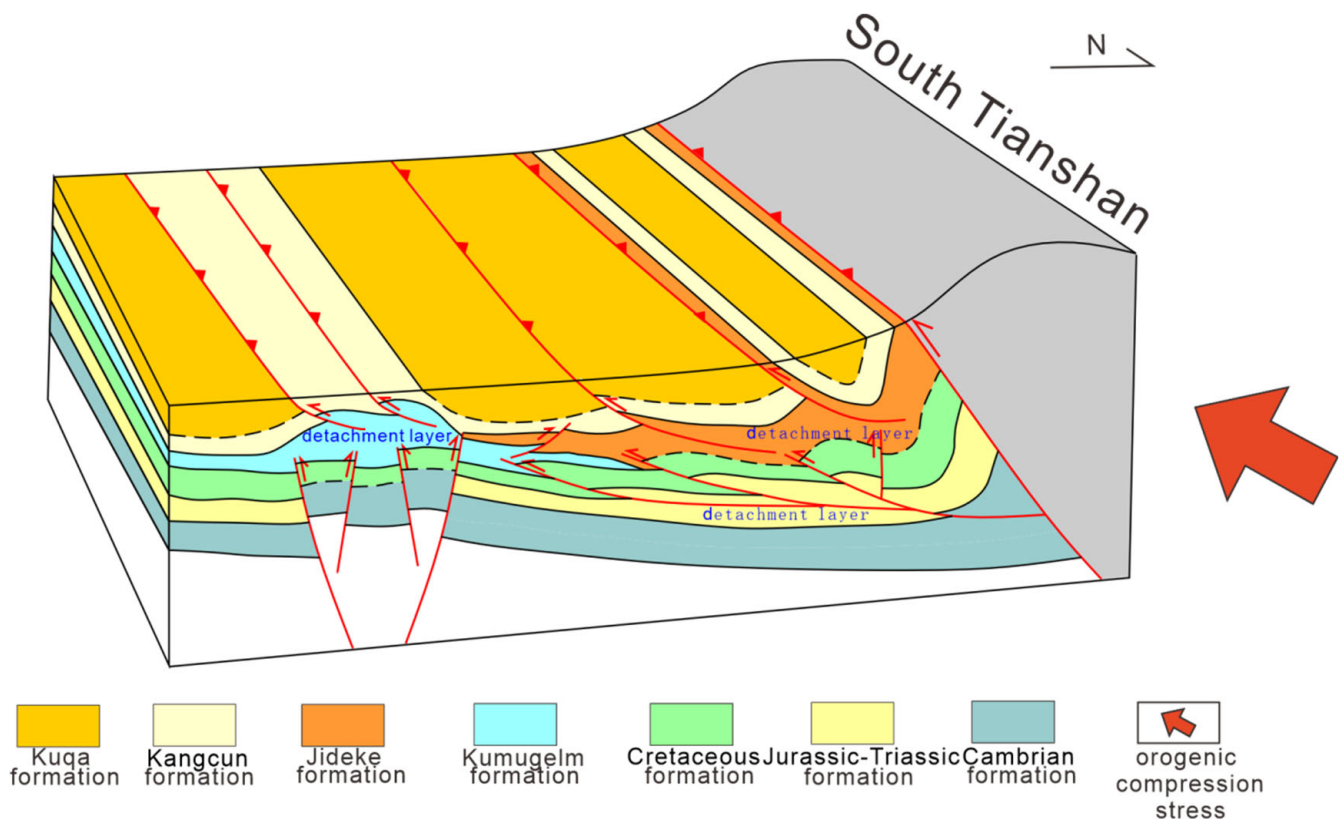


**Figure 14.** Development model map of the Qiulitage fold and thrust belt.

## 6. Conclusions

The QFTB is divided into four segments from west to east based on the differences in the geometric characteristics of the developed salt-related structures. These segments are the West QFTB segment, the Central QFTB segment, the East QFTB segment, and the Dina segment. The West QFTB segment mainly develops salt layers from the Jurassic period, featuring the formation of buried mountain thrust structures. The Central QFTB segment is situated at the convergence zone of two salt lakes, characterized by the development of multiple-row cover detachment thrusts. The East QFTB segment develops salt layers from the Neogene period, with the formation of cover detachment thrusts. The Dina segment features basal-involved thrust faults.

The Xishan period is the main deformation period of the QFTB, with a noticeable trend of decreasing deformation intensity from east to west. In the main deformation period, the shortening rate in the eastern Dina segment can reach 18%, while in the western West QFTB segment, it is only 9%.

The differences in the nature of the detachment layer and the stress field are the main factors leading to the strong segmentation of the QFTB. The type and thickness of the upper detachment layer determine the number of faults in the fault belt, while the thickness of the lower detachment layer determines the development mode of the faults. When the thickness is greater than 800 m, cover detachment thrusts develop. When it is less than 800 m, basal-involved thrust faults develop. In the absence of a lower detachment layer, imbricate thrust faults do not develop. The stress field mainly affects the dip angle of the faults. The horizontal thrust distance should be jointly determined by the detachment layer and stress conditions.

**Author Contributions:** Conceptualization, Y.Z. (Yibo Zhao); Methodology, Y.Z. (Yingzhong Zhu), Y.Z. (Yuhang Zhang) and T.G.; Software, Y.Z. (Yingzhong Zhu); Writing—original draft, Y.Z. (Yingzhong Zhu); Writing—review & editing, C.L. All authors have read and agreed to the published version of the manuscript.

**Funding:** The authors gratefully express their gratitude for the financial support provided by the National Natural Science Foundation of China (No. 42330810). Thanks for the data provided by the Northwest Petroleum Bureau Limited Company.

**Data Availability Statement:** The seismic data underlying our research is for production purposes and is strictly confidential. If there are relevant researchers interested in our research, they can contact us by email.

**Conflicts of Interest:** The authors declare no conflict of interest.

## References

- Adeoti, B.; Alexander, A.; Webb, G. Geomorphology of contractional salt tectonics along the Kuqa fold-thrust belt, northwestern China: Testing pre-kinematic diapir versus source-fed thrust and detachment fold models. *J. Struct. Geol.* **2022**, *161*, 104638. [[CrossRef](#)]
- Yang, K.; Qi, J.; Shen, F.; Sun, T.; Duan, Z.; Cui, M.; Li, P.; Lv, J. formation mechanism of salt piercement structures in a compressive environment: An example from the Kuqa Depression, western China. *J. Struct. Geol.* **2024**, *178*, 105005. [[CrossRef](#)]
- Zhao, H.; Chen, S.; Yuan, H.; Wang, X.; Luo, C.; Wang, F.; Yao, X.; Li, Q. Cenozoic salt-related structural styles and exploration potential: A case of the eastern part of the Qiulitage structural belt in the Kuqa foreland basin. *J. China Univ. Min. Technol.* **2023**, *52*, 113–127.
- Li, C.; Yin, H.; Wu, Z.; Zhou, P.; Wang, W.; Ren, R.; Guan, S.; Li, X.; Luo, H.; Jia, D. Effects of Salt Thickness on the Structural Deformation of Foreland Fold-and-Thrust Belt in the Kuqa Depression, Tarim Basin: Insights from Discrete Element Models. *Front. Earth Sci.* **2021**, *9*, 655173. [[CrossRef](#)]
- Lai, J.; Li, D.; Ai, Y.; Liu, H.; Cai, D.; Chen, K.; Xie, Y.; Wang, G. Structural diagenesis in ultra-deep tight sandstones in the Kuqa Depression, Tarim Basin, China. *Solid Earth* **2022**, *13*, 975–1002. [[CrossRef](#)]
- Luo, L.; Guo, J.; Hu, C.; Lin, H.; Quaye, J.A.; Zhou, X.; Han, B. Sedimentary characteristics and development model of the bedded evaporites in the Paleogene Kumugelm formation, Kuqa Depression, Northwestern China. *Carbonates Evaporites* **2024**, *39*, 68. [[CrossRef](#)]
- Dong, C.; Wei, G.; Liu, M.; Li, D.; Miao, W. Geological Structural Variability and formation Mechanism of the Qiulitage Structural belt in the Kuqa Depression. In Proceedings of the 33rd National Natural Gas Academic Annual Conference, Nanning, China, 1 June 2023.
- Jin, W.; Tang, L.; Wan, G.; Yu, Y.; Wang, Q.; Yang, W.; Peng, G.; Lei, G. Salt-related Structural Characteristics in the Eastern Qiulitage Area of the Kuqa foreland basin. *Acta Pet. Sin.* **2007**, *28*, 8–15.
- Tang, L.; Wan, G.; Wang, Q.; Jin, W.; Yang, W. Mesozoic Structural Evolution of the Western Qiulitage Structural belt in Kuqa. *J. Southwest Pet. Univ. Nat. Sci. Ed.* **2008**, *30*, 167–171.
- Wang, X.; Jia, C.; Yang, S. The Time of Deformation on the Kuqa Fold-and-Thrust Belt in the Southern Tianshan-Based on the Kuqa River Area. *Geol. Sci.* **2002**, *76*, 55–63.
- Qin, P.; Zhong, D.; Su, C.; Mo, T.; Tang, Y. Effect of the internal plastic deformation of salt structures on the lithologic succession of evaporites: A case study on the Palaeogene Kumugelm formation, Kelasu Thrust Belt, Kuqa Depression, Tarim Basin. *J. Pet. Sci. Eng.* **2022**, *208*, 109559. [[CrossRef](#)]
- Wang, W.; Xie, H.; Yin, H.; Jia, D.; Xu, Z.; Luo, H.; He, W.; Yuan, R.; Duan, Y. Structural Variation between the Western and Eastern Kuqa Fold and thrust Belt, China: Insights from Seismic Interpretation and Analog Modeling. *Acta Geol. Sin. Engl. Ed.* **2023**, *97*, 1078–1093. [[CrossRef](#)]
- Yu, H.; Qi, J.; Yang, X.; Liu, Q.; Cao, S.; Fan, S.; Sun, T.; Yang, X. Paleogeographic Analysis of Mesozoic Structures in the Kuqa Depression of the Tarim Basin. *Geol. J. China Univ.* **2016**, *22*, 657–669.
- Li, J.; Li, J.; Xie, Z.; Chao, W.; Zhang, H.; Mancang, L.; Dejiang, L.I.; Wei, M.A.; Danfeng, M. Oil and gas source and accumulation of Zhongqiu 1 trap in Qiulitage structural belt, Tarim Basin, NW China. *Pet. Explor. Dev. Online* **2020**, *47*, 548–559. [[CrossRef](#)]
- Yang, M.; Zhao, Y.; Yan, L.; Li, H.; Zhang, X.; Xu, Z.; Luo, H. Structural features of the eastern Qiulitage Tectonic Belt and petroleum geological significance. *Nat. Gas Geosci.* **2018**, *6*, 826–833.
- Yu, H.; Qi, J.; Yang, X.; Sun, T.; Liu, Q.; Cao, S. Analysis of Mesozoic Prototype Basin in Kuqa Depression, Tarim Basin. *Xinjiang Pet. Geol.* **2016**, *37*, 644–653.
- Wei, H.; Huang, W.; Luo, H.; Li, L.; Shi, L.; Wang, Z. Fault characteristics and tectonic evolution of eastern Kuqa Depression. *Earth Sci.* **2016**, *41*, 1074–1080.
- Xu, W.; Wang, W.; Yin, H.; Jia, D.; Yang, G.; Li, G. Numerical simulation of different subsalstructural features and their evolution in the eastern and western segments of the kuqa Depression. *Acta Geologica Sin.* **2020**, *20*, 1740–1751.

19. Miao, J.; Jia, C.; Wang, Z.; Zhang, J.; Zhao, E. Segmental Structural Characteristics and Hydrocarbon Accumulation in the Qiulitage Structural belt. *Pet. Explor. Dev.* **2004**, *4*, 558–569.
20. Xie, H.; Wu, Z.; Neng, Y.; Yin, H.; Koyi, H. The Influence of the Syn-kinematic Depositional Rate on the Compressional Deformation of Pre-existing Passive Salt Diapir: The Analysis and Analogue Modeling of Salt Structures in the Western Qiulitage Structural Belt, Kuqa Depression. *Geol. J. China Univ.* **2014**, *20*, 611–622.
21. Yin, H.; Wang, Z.; Wang, X.; Wu, Z. Characteristics and formation mechanism of Cenozoic salt structure in Kuqa foreland basin: Physical simulation and discussion. *Geol. J. Univ.* **2011**, *17*, 308–317.
22. Zhang, W.; Xu, Z.; Zhao, F.; Wu, S.; Huang, C.; Zhang, X. Structural Deformation Styles and Tectonic Evolution Characteristics in Eastern Kuqa Depression. *Xinjiang Pet. Geol.* **2019**, *40*, 48–53.
23. Gao, L.; Rao, G.; Tang, P.; Qiu, J.; Peng, Z.; Pei, Y.; Yu, Y.; Zhao, B.; Wang, R. Structural development at the leading edge of the salt-bearing Kuqa fold-and-thrust belt, southern Tian Shan, NW China. *J. Struct. Geol.* **2020**, *140*, 104184. [[CrossRef](#)]
24. Gao, L.; Wang, X.; Rao, G. Two-dimensional balance restoration of salt structures and analysis of restored structural profiles in the western segment of the Kuqa Depression. *Acta Geol. Sin.* **2020**, *94*, 1727–1739.
25. Han, Z.; Zeng, L.; Gao, Z. Difference of structural deformation and reservoirs physical property in Qiulitage structural belt of Kuqa foreland basin. *Nat. Gas Geosci.* **2014**, *25*, 508–515.
26. Wan, G.; Tang, L.; Jin, W.; Yu, Y. Analysis of Cenozoic Structural Evolution in the Western Qiulitage Structural belt of the Kuqa Depression. In Proceedings of the 4th International Symposium on Petroleum formation Mechanism and Resource Assessment, Lisbon, Portugal, 19–25 May 2006.
27. Zhang, L.; Yang, X.; Huang, W.; Yang, H.; Li, S. Fold segment linkage and lateral propagation along the Qiulitage anticline, South Tianshan, NW China. *Geomorphology* **2021**, *381*, 107662. [[CrossRef](#)]
28. Duan, Y.; Luo, H.; Xe, H.; Xu, Z.; Zhang, X.; Zhang, J.; Lei, S.; Rui, Y. Salt-related structural characteristics and deformation mechanism Dongqiu section of the Qiulitage structural belt, Tarim Basin. *Nat. Gas Geosci.* **2021**, *32*, 993–1008.
29. He, W.; Wang, W.; Xie, H.; Yin, H.; Jia, D.; Xu, Z.; Luo, H.; Yuan, R. The effects of salt flow on the cross-section restoration of salt-bearing fold-and-thrust belts: An example from the Kuqa Depression. *J. Struct. Geol.* **2023**, *167*, 104795. [[CrossRef](#)]
30. Ju, W.; Zhong, Y.; Liang, Y.; Gong, L.; Yin, S.; Huang, P. Factors influencing fault-propagation folding in the Kuqa Depression: Insights from geomechanical models. *J. Struct. Geol.* **2023**, *168*, 104826. [[CrossRef](#)]

**Disclaimer/Publisher's Note:** The statements, opinions and data contained in all publications are solely those of the individual author(s) and contributor(s) and not of MDPI and/or the editor(s). MDPI and/or the editor(s) disclaim responsibility for any injury to people or property resulting from any ideas, methods, instructions or products referred to in the content.